A. Altun / Hacettepe J. Biol. & Chem., 2025, 53 (1), 159-168

Research Article

Hacettepe Journal of Biology and Chemistry

journal homepage: https://hjbc.hacettepe.edu.tr/
Dergipark Akademik: https://dergipark.org.tr/en/pub/hjbc

Schiff Base-Nickel(Iı) Complex: A Robust Luminescent Probe For The Detection Of 2,4,6-Trinitrophenol İn An Aqueous Medium

Schiff Bazı-Nikel(II) Kompleksi: Sulu Ortamda 2,4,6-Trinitrofenol Tespiti Için Güçlü Bir Lüminesans Probu

Ayhan Altun
Department of Chemistry, Gebze Technical University, Kocaeli, Turkey.

ABSTRACT

This study delved into the fluorescence properties of a Ni(II) Schiff base complex towards nitroaromatic compounds, such as dinitrobenzene (DNB), 2,4,6-trinitrotoluene (TNT), 2,4-dinitrotoluene (DNT), 2-nitrophenol (2-NP), 4-nitrophenol (4-NP), 2,4-dinitrophenol (DNP), and 1,3,5-trinitrophenol (TNP),. Remarkably, the compound exhibited exceptional sensitivity in detecting TNP, with a notable Ksv value of 40.5×10^3 M^{-1} . LOD value of the targeted compound was found to be 0.134 µM, encompassing a linear working range of 2.50–50.00 µM.. Furthermore, the synthesized Ni(II) complex proved effective in the fluorescence quenching-based detection of TNP in water solutions, demonstrating both high selectivity and sensitivity. Through fluorescence titrations (Job's plot), the stoichiometry between the compound and TNP was found to be 2/1 (complex/TNP). This finding underlines the potential utility of the complex as a promising tool in environmental monitoring or related fields where the detection of TNP is crucial.

Key Words
Fluorescent sensor, Schiff base-Ni complex, nitroaromatic compounds, TNP.

ÖZ

Bu çalışmada, bir Ni(II) Schiff baz kompleksinin floresans özellikleri incelenmiştir. Bu kompleksin dinitrobenzen (DNB), 2,4,6-trinitrotoluen (TNT), 2,4-dinitrotoluen (DNT), 2-nitrofenol (2-NP), 4-nitrofenol (4-NP), 2,4-dinitrofenol (DNP) ve 1,3,5-trinitrofenol (TNP) gibi nitroaromatik bileşiklere karşı sensör kabiliyetleri, floresans spektroskopisi kullanılarak ayrıntılı bir şekilde araştırılmıştır. Bileşik, 40.5×10^3 M^{-1}'lik kayda değer bir Ksv değeri ve 2.50-50.00 µM'lik doğrusal bir çalışma aralığını kapsayan 0.134 µM'lik etkileyici derecede düşük bir LOD ile TNP'yi tespit etmede olağanüstü bir hassasiyet sergilemiştir. Araştırma, [NiLCl(H2O)2]·2H2O kompleksinin güçlü floresans özellikler gösterdiğini ortaya koymuştur. Ayrıca, bu sentezlenmiş Ni(II) kompleksi, sulu çözeltilerinde TNP'nin floresans söndürme esasına dayalı tespitinde hem yüksek seçicilik hem de hassasiyet göstermiştir. Floresans titrasyonları (Job's plot) aracılığıyla yapılan analizler, kompleks ve TNP arasındaki stokiyometrinin 2:1 (kompleks/TNP) olduğununu göstermiştir. Bu bulgular, TNP'nin tespitinin kritik olduğu çevresel izleme veya ilgili alanlarda bu kompleksin umut verici bir araç olarak potansiyel kullanımını vurgulamaktadır.

Anahtar Kelimeler
Floresans sensör, Schiff bazlı- Ni kompleksi, nitroaromatik bileşikler, TNP.

Article History: Jul 5, 2024; Accepted: Sep 30, 2024; Available Online: Dec 21, 2024.
DOI: https://doi.org/10.15671/hjbc.1511046
Correspondence to: A. Altun, Department of Chemistry, Gebze Technical University, Kocaeli, Turkey.
E-Mail: altun@gtu.edu.tr

INTRODUCTION

In recent decades, the detection of nitro-containing high-energy nitroaromatic organic compounds (NACs) include TNP, TNT, and DNT has gained considerable attention due to its crucial role in biological and environmental process (1). TNP, also recognized as picric acid (PA), is one the most important class of nitroaromatic organic compounds because of its applicantionin industries such as leather, pharmaceuticals, dyes as well as in the manufacturing of explosives and fireworks. The notable solubility of TNP in water facilitates its dispersion into water bodies and soil, culminating in significant environmental contamination and degradation (2). The enduring presence of TNP in the environment, owing to its resistance to biological breakdown attributed to its electron-withdrawing nitro groups, underscores the gravity of the issue (3, 4). Moreover, the toxicity and mutagenicity of TNP pose grave risks to both human and wildlife populations (5, 6). Exposure to TNP, whether through inhalation or skin contact, can lead to various health complications ranging from dermatitis to severe afflictions such as chronic liver and kidney poisoning, and in extreme cases, fatalities. Hence, the precise identification of TNP holds paramount importance for safeguarding human health and preserving environmental integrity.

Various techniques are employed for detecting explosives, for instance, mass spectrometry (7) , ion mobility spectrometry (8), gas chromatography (9), surface-enhanced Raman scattering (10) infrared spectroscopy (11), fluorescence spectroscopy (12-14), colorimetric analysis (15), electrochemical analysis (16) and electrophoresis (17), . Among these, fluorescence-based sensors have gained prominence for their remarkable sensitivity, rapid response times, precise selectivity, real-time monitoring capabilities, and user-friendly operation. Over the last decade, there has been a surge in the development and exploration of fluorescent sensors tailored for nitro explosive detection.

These sensors encompass a diverse array of materials, including conjugated polymers (18-22) porous metal-organic frameworks (MOFs) (23-27), covalent organic frameworks (COFs) (28), luminescent gels (29), organic-inorganic hybrid materials (30), and Schiff bases (31). Schiff bases are an important class of ligands due to their structural versatility, straightforward synthesis, and capacity to form stable complexes (32, 33). Due to their distinctive photophysical and chemical properties, Schiff bases can be used in a variety of research areas including medicinal and analytical chemistry (34, 35).

The central aim of the current study lies in the re-synthesis and investigation of the photophysical properties of a Schiff base complex, as previously reported by Turan and collaborators (32, 36). It has been well-established that the Schiff base Ni(II) complex exhibits distinctive fluorescence sensor attributes, particularly in its sensitivity to TNP. Consequently, the targeted Ni(II) complex emerges as a promising candidate for serving as a sensor specifically tailored for the detection of TNP.

Experimental

Procedure for fluorescence sensing of TNP

Fluorescence quenching titration experiments were conducted in water by gradually increasing the concentration of TNP (2,5-50 µM) within a micro quartz cuvette, while maintaining the concentration of the Ni(II) complex at 15 µM. For each addition, a minimum of three fluorescence spectra were recorded. The excitation wavelength (ex.) of 380 nm was chosen for the compound, utilizing a 5 nm slit width.

The relationship between the fluorescence emission intensity (I_0/I) and the increasing concentration of the quencher ([Q]) was accurately described by the Stern–Volmer equation: $I_0/I = 1 + K_{SV}[Q]$. Here, K_{SV} represents the Stern–Volmer quenching constant, which was determined from the slope of the Stern–Volmer plot.

The luminescence spectra of the Ni(II) complex were investigated in various solvents as follows: Samples of the Ni(II) complex at a concentration of 15 µM were prepared by grinding and dispersing them in 2.0 mL of each solvent (H_2O, DMF, DMSO, EtOH, MeOH, ACN, DCM, acetone, and hexane). The suspensions were then transferred into quartz cuvettes for the experiments.

Additionally, the fluorescence response against NACs was studied in the presence of the Ni(II) complex at a predetermined concentration and solvent system of 15 µM. Photophysical characteristics and fluorescent sensor performance were assessed using UV–Vis absorption and fluorescence measurements.

Result and Discussion

In this study, we introduce a novel fluorescent sensor based on a water-soluble Schiff base-derived Ni(II) complex which exhibits exceptional sensitivity and selectivity for spectrofluorimetric detection of TNP in aqueous solutions. In order to evaluate its efficacy, the photophysical and fluorescent sensor properties of the targeted compound were examined by using UV-Vis absorption and fluorescence methods.

Furthermore, the experimental parameters were optimized to enhance the spectrofluorimetric detection of TNP in fully aqueous environments. By fine-tuning these parameters, we aimed to maximize the sensors efficiency in detecting TNP with high precision.

Additionally, we investigated the analytical capabilities of the Ni(II) complex, particularly its fluorescence response when transitioning to the 'turn-off' mode upon exposure to TNP. This assessment provides valuable insights into the sensors performance and its potential application in real-world detection scenarios.

The optical properties of the Ni(II) complex were assessed at room temperature using both UV–Vis and fluorescence spectroscopies. To comprehensively understand its absorption behavior, solutions of the Ni(II) complex at a concentration of 15 µM were prepared in various solvents, including water, acetone, dimethylformamide, ethanol, methanol, acetonitrile, dichloromethane, dimethyl sulfoxide, and n-hexane (Fig. 1d). As illustra-

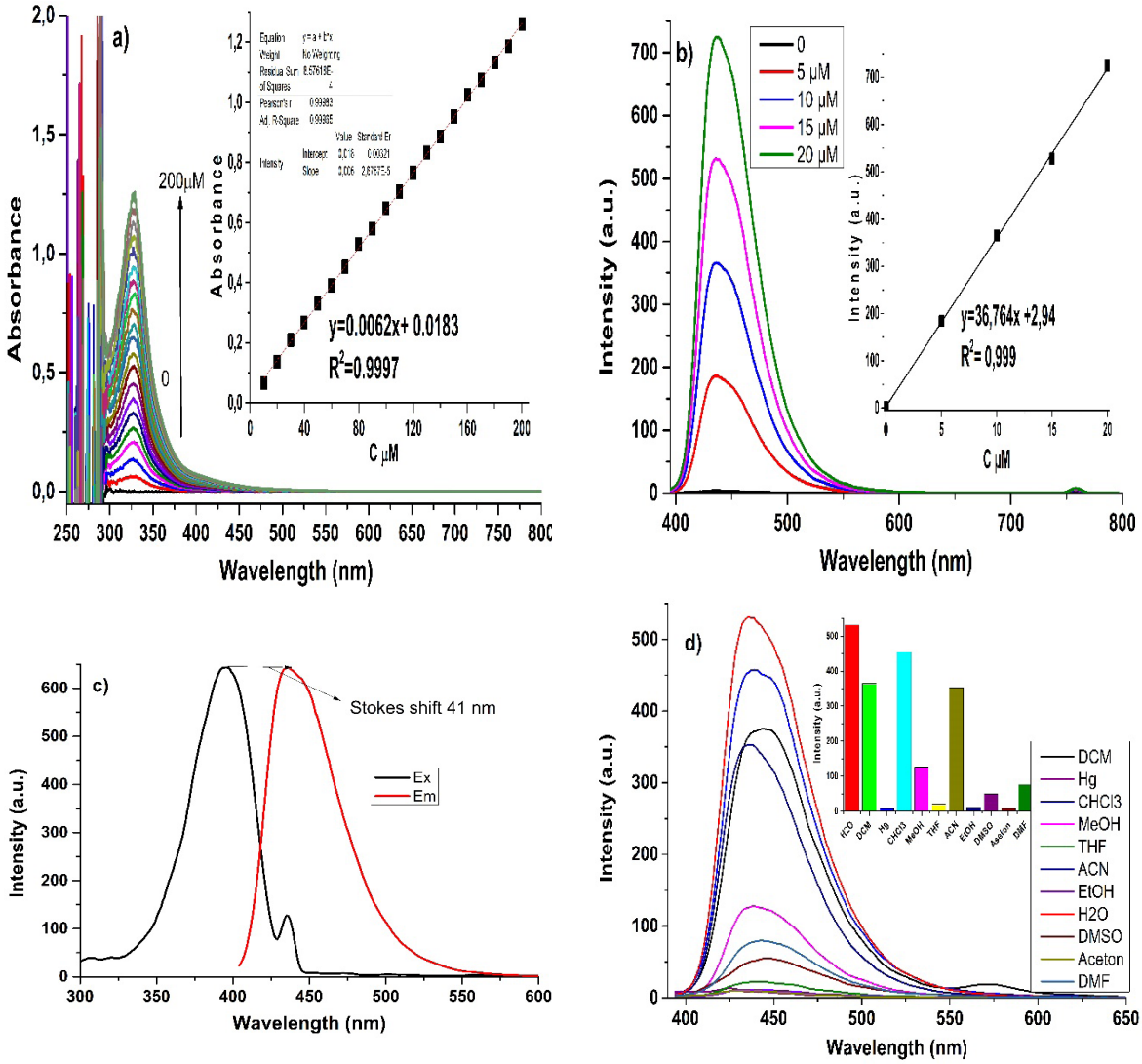

Figure 1. a) UV–Vis absorption, b) fluorescence signal, c) stokes shift in water, d) fluorescence spectra of complex in various solvent systems.

ted in Fig. 1a, the Ni(II) complex displayed distinctive absorption peaks centered at 330 nm, corresponding to the π—π* transition (37). Remarkably, these findings revealed the solvent-independent absorption characteristics of the Ni(II) complex. Additionally, the absorption behavior of the Ni(II) complex at different concentrations ranging from 5 to 20 µM in aqueous media was studied. This investigation provided further insights into the concentration-dependent absorption properties of the complex in a relevant solvent environment.

The fluorescence emission properties of the Ni(II) complex were investigated using fluorescence spectroscopy with excitation at 380 nm. As depicted in Fig. 1b, the Ni(II) complex displayed a strong blue fluorescence emission, peaking at around 436 nm, accompanied by a calculated Stokes shift of 41 nm (Fig. 1c).

After assessing the photophysical attributes of the Ni(II) complex, we compiled additional parameters pertaining to its photophysical behavior, including molar absorptivity (Ɛ) ($L.mol^{-1}.cm^{-1}$) $x10^3$, and lifetimes (τ_0), which are detailed in Table 1.

Investigation of fluorescent sensor properties

One crucial aspect of developing novel fluorescence sensors lies in achieving a high degree of selectivity for accurately analyzing fluorescence signals within samples. To gauge the selectivity of the sensor under examination, assessments were conducted utilizing UV-Vis and fluorescence measurements in an aqueous medium.

In particular, a solution containing various nitroaromatic compounds (DNB, TNT, 4-NP, 2-NP, DNT, DNP, and TNP) was exposed to a 15 µM solution of the Ni(II) complex, and the UV-Vis responses of the Ni(II) complex were meticulously recorded (as depicted in Fig. 2).

As shown in Fig. S3b, it is evident that the UV–Vis spectroscopic analysis following the incorporation of DNP and TNP into the solution revealed a significant increase in the absorbance of the Ni(II) complex initially centered at 396 nm.

This observation underscores the exceptional selectivity of the Ni(II) complex, which distinctly responded to DNP and TNP among the array of aromatic compo-

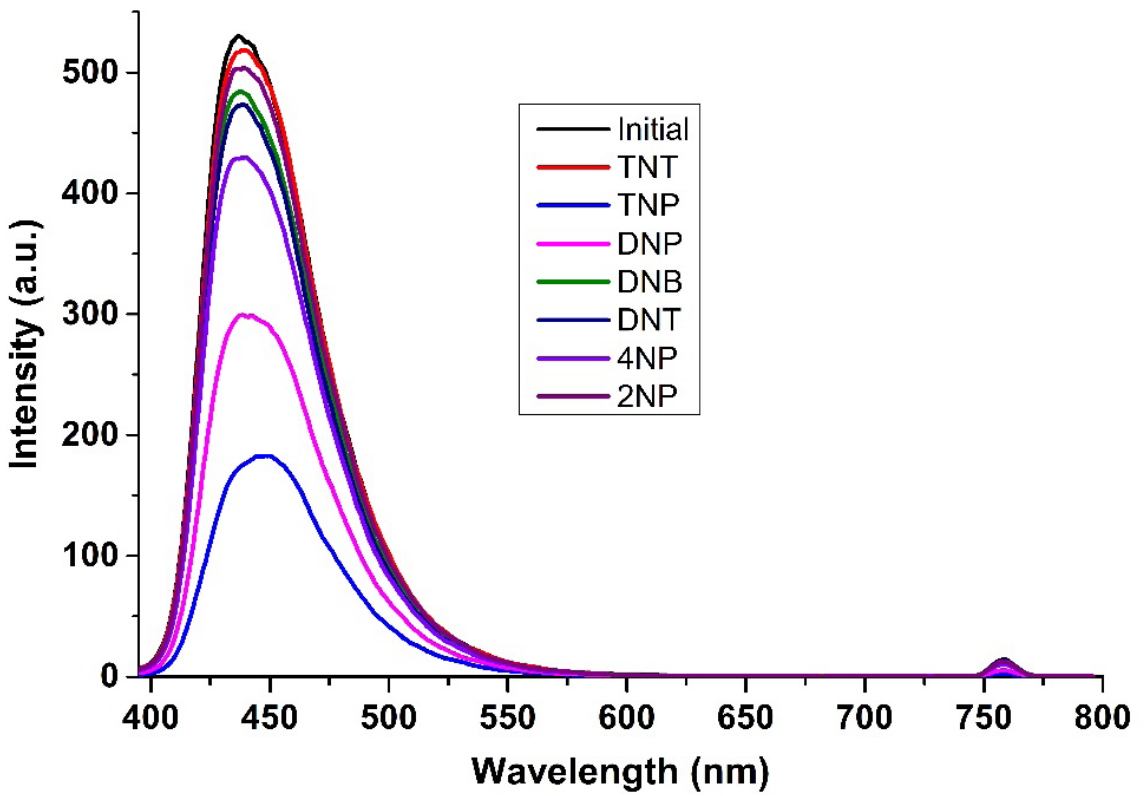

Figure 2. Fluorescence signal, and image of 15 µM Ni(II) complex upon addition of 3 equivalents of different analytes in water.

unds examined. Notably, this selectivity demonstrated a clear correlation with the number of nitro groups present (38). The observed shifts in the UV-Vis absorption spectra subsequent to the introduction of DNP and TNP could be attributed to electronic structural reconfigurations within the Ni(II) complex (Fig. S3b). These alterations are likely instigated by efficient charge transfer mechanisms between the electron-deficient nitroaromatic compounds and the electron-rich Ni(II) complex (39).

After completing the UV-Vis absorption measurements, we proceeded to evaluate the selectivity of the Ni(II) complex concerning TNP using fluorescence spectroscopy, all within the same experimental framework (Fig. 2).

At a concentration of 15 µmol/L, the Ni(II) complex displayed minimal alterations in its fluorescence response when exposed to the various tested nitroaromatic compounds. However, upon the introduction of DNP and TNP, a substantial decrease in fluorescence intensity was observed, resulting in 43.6% and 67.4% fluorescent "turn-off" responses at 436 nm for the Ni(II) complex (Fig. S3).

These results emphasize the outstanding selectivity of the Ni(II) complex for TNP, even in the presence of competing nitroaromatic compounds that may be present in the sample matrix. Furthermore, it was observed that the magnitude of the fluorescence "turn-off" response increased proportionally with the degree of nitration present within the molecules.

The heightened response to TNP compared to DNP can be attributed to the superior electron-accepting nature of TNP, stemming from the higher number of nitro groups attached to its phenol unit.

In our study, we conducted interference using a 15 µmol/L solution of Ni(II) complex in water, and various nitroaromatic compounds (DNB, TNT, 4-NP, 2-NP, and DNT) at a concentration of 15.00 µM. The evaluation was based on the relative changes in fluorescence signals, as depicted in Fig. 2. This robust selectivity, especially against TNP, was maintained. The discernible occurrence of efficient electron transfers processes between the fluorescent sensor and TNP was selectively initiated, resulting in notable fluorescent 'turn-off' responses observed at 436 nm for the Ni(II) complex in the aqueous medium. Consequently, it can be concluded that the spectrofluorimetric determination of trace concentrations of TNP can be reliably executed using the presented fluorescent sensor (Ni(II) complex) in a 100% aqueous environment, even when coexisting with other competitive species.

To further understand the selectivity of Ni(II) complex, a visual detection test was conducted using 380 nm irradiation (Fig. 2a). The color of Ni(II) complex shifted from a vibrant blue to colorless upon the addition of TNP, while competitive species failed to induce any color change in the solutions. These results unequivocally affirm that Ni(II) complex holds significant promise as a candidate for the highly sensitive, efficient, and selective determination of TNP using spectrofluorimetry.

In the realm of spectrofluorimetric analysis, it is crucial for both the fluorescence sensor utilized and the resulting guest-host configuration to possess robust chemical stability, ensuring the consistent and precise acquisition of data. Consequently, we conducted an investigation into the photostability of the complex formed by Ni(II) complex (at a concentration of 15 µmol/L) and TNP (at a concentration of 22.00 mg/L) in an aqueous environment, referred to as Ni(II) complex + TNP. This assessment involved observing the fluctuations in fluorescence signals over a duration of 0 to 100 minutes under natural light conditions, as illustrated in Fig. 3.

It was revealed that the fluorescence signals of both the Ni(II) complex and the Ni(II) complex + TNP complex remained virtually unchanged throughout the 100-minute duration. This observation highlights the remarkable photostability demonstrated by both entities, emphasizing their resilience to degradation under prolonged exposure to light.

The interaction and sensing mechanism involving the Ni(II) complex with TNP

The chemical stoichiometry of the interaction between Ni(II) complex and TNP through was examined through Job's plot analysis, specifically utilizing the continuous variation method in an aqueous solution. Employing a concentration of 15 µmol/L of Ni(II) complex, the mole fraction of TNP in the resulting Ni(II) complex + TNP complex was incrementally varied in the aqueous medium. As illustrated in Fig. 4a, the fluorescence signal of the complex peaked at a mole fraction of TNP within the Ni(II) complex + TNP structure of 0.30. This

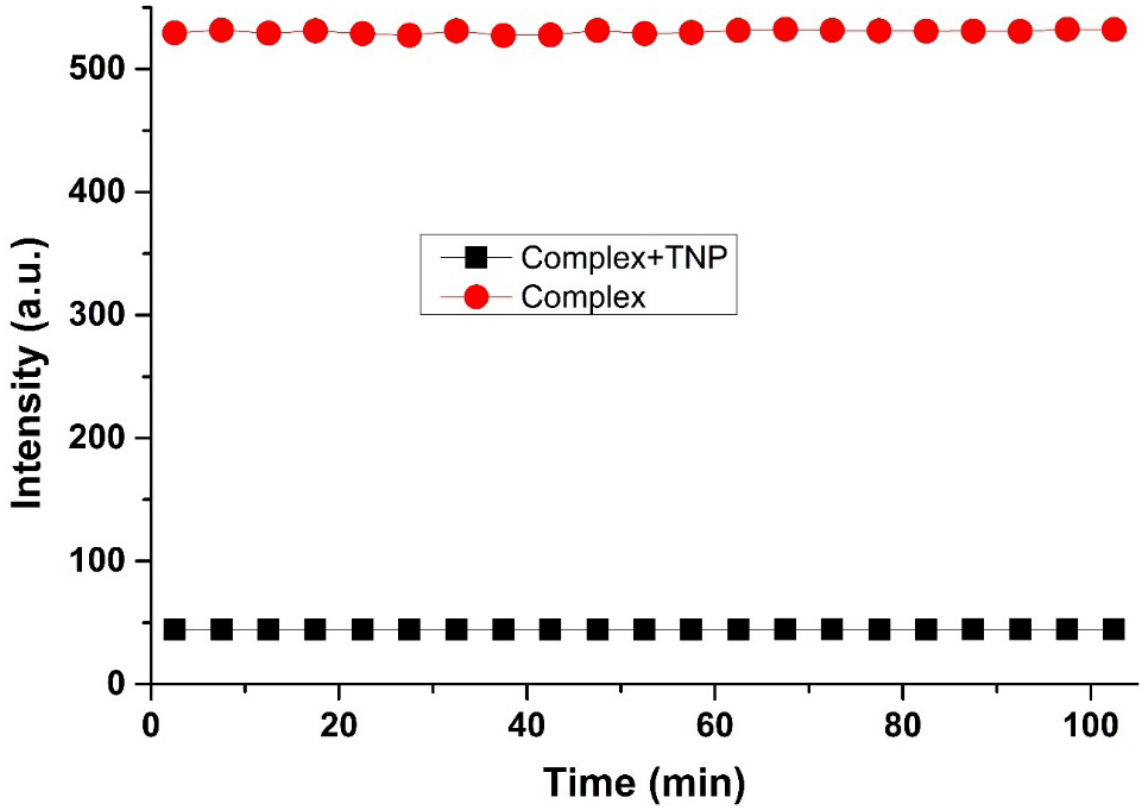

Figure 3. Photostability of Ni(II) complex and Ni(II) complex + TNP in water (λex=380 nm, λem=436 nm).

observation strongly indicates a stoichiometry of 2:1 (host:guest ratio) for the Ni(II) complex + TNP complex.

Furthermore, the association constant for the formation of the TNP complex with Ni(II) complex in water was determined to be 1.12×10^7 M^{-1} using the Benesi-Hildebrant equation. This determination was made by employing a 15 µmol/L concentration of Ni(II) complex while gradually increasing the amount of TNP, as shown in Fig. 4b.

To confirm the binding ratio, we utilized non-linear curve fitting analysis, as depicted in Fig. 4c, by incrementally introducing TNP to the Ni(II) complex. This analysis identified an inflection point at a 2:1 (host:guest) ratio, indicating the binding stoichiometry between TNP and the Ni(II) complex (Fig. 4a). The results from both the Job's plot and the non-linear curve fitting analysis are in agreement and corroborate each other.

Moving forward, we delved into the fluorescence quenching mechanism of Ni(II) complex following its interaction with TNP. This investigation was crucial as it is well-known that sensor systems exhibit either static or dynamic quenching processes. These two quenching mechanisms are fundamentally different: dynamic quenching relies on the collision of the quencher with the excited fluorophores, whereas non-radiative complex formation accounts for static quenching (40).

Subsequently, after the interaction between Ni(II) complex and TNP, the Stern–Volmer equation (Eq. (1)) was applied to explore the fluorescence quenching mechanism.

$$I_0/I = Ksv[Q] + 1 \quad (1)$$

After plotting the I_0/I against [Q], a linear graph emerged with a y-axis intercept at 1, signifying the presence of static quenching. However, as the quencher concentration increased, the linear graph displayed positive deviation, indicating the influence of dynamic quenching on the fluorescence quenching mechanism (41). Fig. 6a. illustrates that the Stern-Volmer plot for Ni(II) complex, following its interaction with TNP, displayed a y-axis intercept at 1. However, as the TNP concentration increased, the linear graph displayed a positive deviation, indicating that the fluorescence signal was significantly

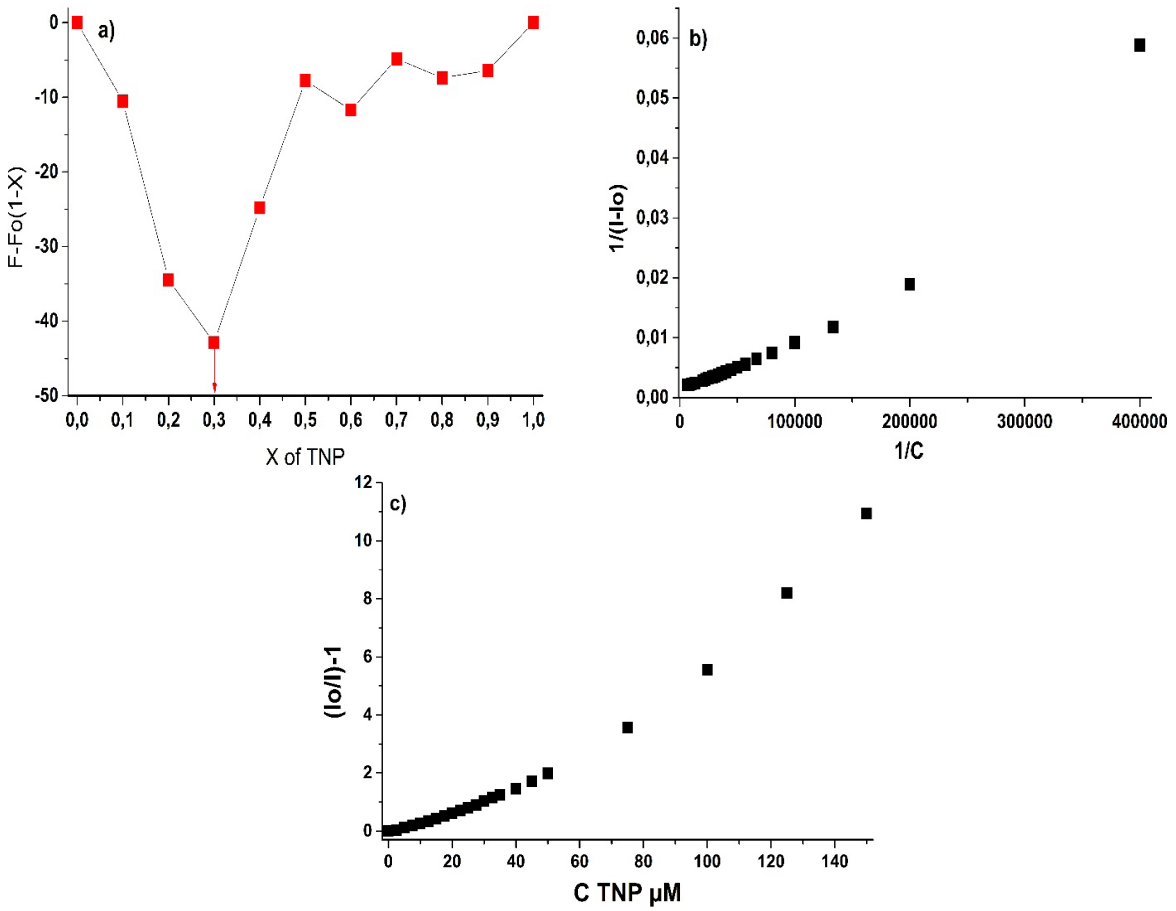

Figure 4. a) Job's plots graph, b) Benesi-Hildebrant graph, c) nonlinear curve for Ni(II) complex + TNP in water.

quenched by both dynamic and static quenching mechanisms.

The time-resolved fluorescence spectroscopy was used to further investigate the fluorescence quenching mechanism in sensor systems. This technique offers detailed insights as fluorescence lifetimes undergo negligible changes in static quenching but significantly decrease in dynamic quenching. In static quenching, the fluorescence lifetime ratio (τ0 in the absence of analyte and τ in its presence) should remain close to 1 due to non-fluorescent complex formation (42).

In our study, the fluorescence lifetimes of Ni(II) complex and Ni(II) complex + TNP were measured under optimized conditions, resulting in values of 4.500 ± 0.006 (τ_0) and 4.465 ± 0.006 (τ), respectively (Fig. 5.). This experimental data corroborated that non-fluorescent complex formation was the primary cause of the fluorescence quenching response of Ni(II) complex, as the fluorescence lifetime ratio remained close to 1.

Analytical parameters for TNP determination

To demonstrate the practical application of our fluorescent sensor (Ni(II) complex), we conducted spectrofluorimetric measurements of TNP in water samples. This involved fluorescence titration experiments where we systematically increased the concentration of TNP while monitoring the fluorescence of the Ni(II) complex under optimized conditions, as shown in Fig. 6a. The fluorescence signal of the Ni(II) complex, peaking at 436 nm, exhibited a significant and proportional decrease ('turn-off' response) in aqueous solutions, particularly up to a TNP concentration of 15.00 mg/L. We established a linear relationship between the TNP concentration and the response of the Ni(II) complex, demonstrating its potential as a quantitative sensing tool.

In Fig. 6b, it is clear that the relative fluorescence signal of the Ni(II) complex demonstrated a robust linear relationship within the TNP concentration range of 2.5 to 50.0 µM. We determined a linear regression equation

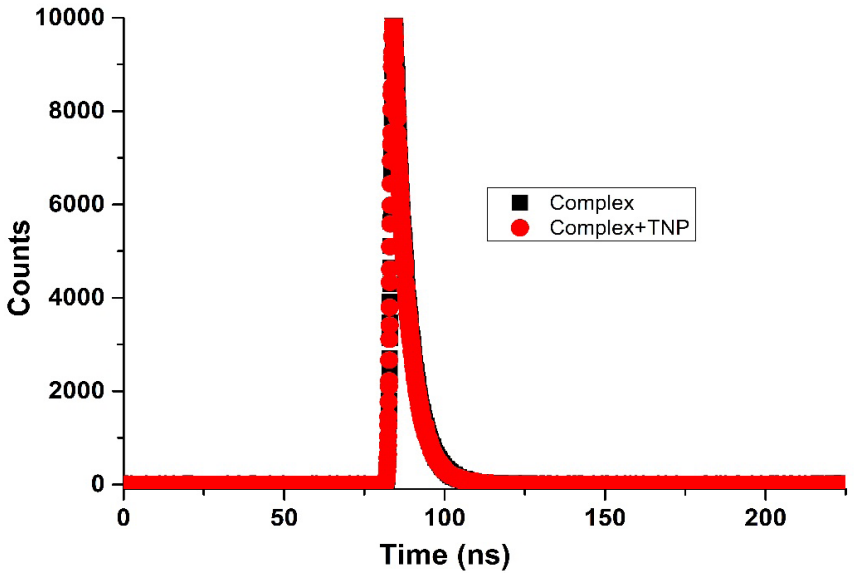

Figure 5. The fluorescence decay profiles of the Ni(II) complex were examined in the presence of TNP, employing a laser excitation source emitting at 390 nm.

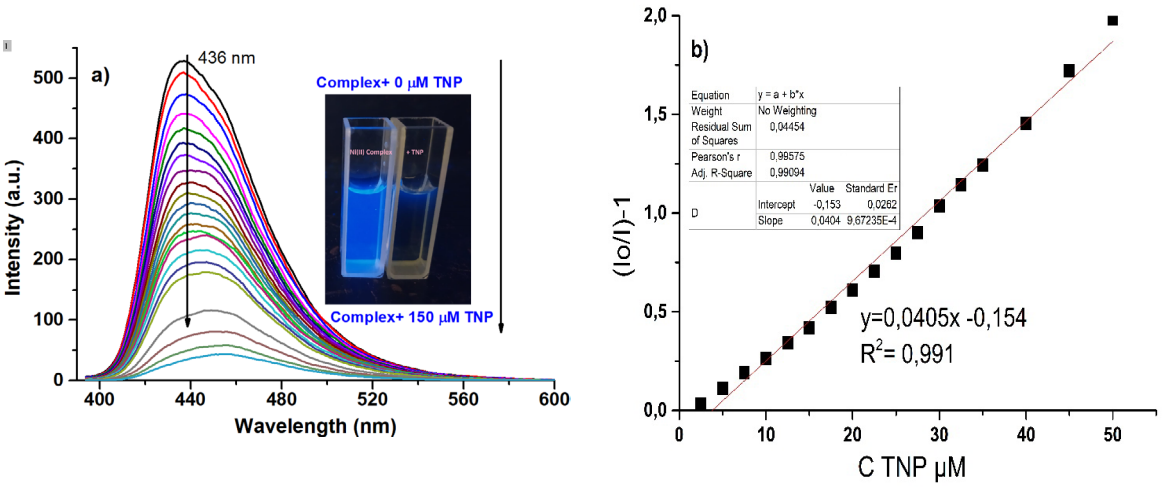

Figure 6. a) The fluorescence titration, and inset: under 365 nm UV lamp and b) illustrates the linear relationship (λex = 380 nm and 15 µM of Ni(II) complex).

Table 1. Analytical parameters for Ni(II) complex in aqua.

Analytical parameters	Ni(II) complex
Ɛ (L.mol^{-1}.cm^{-1}) x10^3	6.9
Excitation wavelength (nm)	380
Emission wavelength (nm)	436
Linear range (µM)	2.5-50
Sensor concentration (µM)	15
Ksv (1/M)	40.5 10^3
Correlation coefficient (R^2)	0.991
STD	0.0018
Limit of detection (LOD) (µM)	0.136
Limit of quantification (LOQ) (µM)	0.454

for TNP as y = 0.0405[TNP] - 0.154 (R^2 = 0.991) based on the change in relative fluorescence signal of the Ni(II) complex. This approach highlights the sensor's effectiveness in quantifying TNP in aqueous samples.

The limits of detection (LOD) and quantification (LOQ) for TNP using the Ni(II) complex were also determined. The calculated values were 0.136 µmol/L for LOD and 0.454 µmol/L for LOQ, determined by employing the 3,3σ/K and 10σ/K criteria, respectively. Notably, these LOD and LOQ values are significantly lower than those reported in previous studies involving fluorescent sensors (3, 31, 42-44). This highlights the remarkable sensitivity, consistency, and specificity of our spectrofluorimetric method for TNP detection in purely aqueous media. Detailed analytical parameters are summarized in Table 1.

Conclusion

The synthesized Ni(II) Schiff base complex exhibited remarkable sensor capabilities towards various nitroaromatic compounds, distinctly highlighting its extraordinary sensitivity towards TNP with high Stern-Volmer constant (Ksv: 40.5 × 10^3 M^{-1}) and 2.5- 50 µM linearity with an impressive LOD of 0.136 µM.

The complex, denoted as $[NiLCl(H_2O)_2]\cdot 2H_2O$, exhibited robust fluorescence properties, paving the way for its application in fluorescence quenching-based TNP detection in water solutions. Notably, the complex displayed both high selectivity and sensitivity in detecting TNP.

Insights from fluorescence titrations, particularly through Job's plot analysis, the specific interaction stoichiometry between the compound and TNP was found to be at a 2:1 ratio (ligand/TNP). This finding indicates that two molecules of the complex are involved in association with one molecule of TNP during their interaction, providing crucial information about the nature of the complex-TNP interaction mechanism.

Declaration of competing interest

There are no conflicts to declare.

References

1. E.V. Verbitskiy, G.L.Rusinov, O.N. Chupakhin, V.N. Charushin, Design of fluorescent sensors based on azaheterocyclic push-pull systems towards nitroaromatic explosives and related compounds: A review, Dyes and Pigments, 180 (2020) 108141.
2. Y.F. Zhao, L.B. Xu, F.L. Kong, L. Yu, Design and preparation of poly(tannic acid) nanoparticles with intrinsic fluorescence: A sensitive detector of picric acid, Chem. Eng. J., 416 (2021) 129090.
3. Y.C. Zheng, S. Wang, R.F. Li, L. Pan, L.Q. Li, Z.P. Qi, et al., Highly selective detection of nitroaromatic explosive 2,4,6-trinitrophenol (TNP) using N-doped carbon dots, Res. Chem. Intermediat, 47 (2021) 2421-2431.
4. J.F. Wyman, M.P. Serve, D.W. Hobson, L.H Lee, D.E. Uddin, Acute toxicity, distribution, and metabolism of 2,4,6-trinitrophenol (picric acid) in Fischer 344 rats, J. of Toxicology and Environ. Health, 7 (1992) 313-327.
5. J.F. Wyman, H.E. Guard, W.D. Won, J.H. Quay, Conversion of 2,4,6-Trinitrophenol to a Mutagen by Pseudomonas-Aeruginosa, App. and Environ. Microbiology, 37 (1979) 222-226.
6. D.T.T. Trinh, W. Khanitchaidecha, D. Channei, A. Nakaruk, Synthesis, characterization and environmental applications of bismuth vanadate, Research on Chem. Intermediates, 45 (2019) 5217-5259.
7. T.P. Forbes, E. Sisco, Recent advances in ambient mass spectrometry of trace explosives, Analyst, 143 (2018) 1948-1969.
8. J.S. Caygill, F. Davis, S.P.J. Higson, Current trends in explosive detection techniques. Talanta, 88 (2012) 14-29.
9. J.W. Grate, R.G. Ewing, D.A. Atkinson, Vapor-generation methods for explosives-detection research. Trac-Trends in Anal. Chem., 41 (2012) 1-14 .
10. R. Gillibert, J.Q. Huang, Y. Zhang, W.L. Fu, M.L. de la Chapelle, Explosive detection by Surface Enhanced Raman Scattering, Trac-Trends in Anal. Chem., 105 (2018) 166-172.
11. P. Wen, M. Amin, WD. Herzog, RR. Kunz, Key challenges and prospects for optical standoff trace detection of explosives, Trac-Trends in Anal. Chem., 100 (2018) 136-144.
12. X.C. Sun, Y. Wang, Y. Lei, Fluorescence based explosive detection: from mechanisms to sensory materials, Chem. Society Rev., 44 (2015) 8019-61.
13. C.P. Wang, WW. Sheng, C. Sun, J. Lei, JS. Hu, A cobalt-coordination polymer as a highly selective and sensitive luminescent sensor for detecting 2,4,6-trinitrophenol, Mol. Crystals and Liquid Crystals, 768 (2024) 117-26.
14. J.N. Malegaonkar, M. Al Kobaisi, P. K. Singh, S.V. Bhosale, S.V. Bhosale, Sensitive turn-off detection of nitroaromatics using fluorescent tetraphenylethylene phosphonate derivative, J. of Photochem. & Photobio. A: Chemistry 438 (2023) 114530.
15. Y. Salinas, R. Martínez-Máñez, M.D. Marcos, F. Sancenón, A.M. Costero, M. Parra, et al., Optical chemosensors and reagents to detect explosives, Chem. Soc. Rev., 41 (2012) 1261-96.
16. H.A. Yu, D.A. DeTata, S.W. Lewis, D.S. Silvester, Recent developments in the electrochemical detection of explosives: Towards field-deployable devices for forensic science, Trac-Trends in Anal. Chem., 97 (2017) 374-384.

17. M. Calcerrada, M. González-Herráez, C. García-Ruiz, Recent advances in capillary electrophoresis instrumentation for the analysis of explosives, Trac-Trends in Anal. Chem., 75 (2016) 75-85.
18. D.T. McQuade, A.E. Pullen, T.M. Swager, Conjugated polymer-based chemical sensors, Chem. Rev., 100 (2000) 2537-2574.
19. A. Rose, Z.G. Zhu, C.F. Madigan, T.M. Swager, V. Bulovic, Sensitivity gains in chemosensing by lasing action in organic polymers, Nature, 434 (2005) 876-879.
20. V. Kumar, B. Maiti, M.K. Chini, P. De, S. Satapathi, Multimodal Fluorescent Polymer Sensor for Highly Sensitive Detection of Nitroaromatics, Scientific Reports, 9 (2019) 7269.
21. M.J. Tsai, C.Y. Li, J.Y. Wu, Luminescent Zn(ii) coordination polymers as efficient fluorescent sensors for highly sensitive detection of explosive nitroaromatics, Crystengcomm, 20 (2018) 6762-6774.
22. A. Altun, R.M. Apetrei, P. Camurlu, Functional Biosensing Platform for Urea Detection: Copolymer of Fc-Substituted 2,5-di(thienyl)pyrrole and 3,4-ethylenedioxythiophene, J. of the Electrochem. Soc., 168 (2021) 067513.
23. M. Chhatwal, R. Mittal, R.D. Gupta, S.K. Awasthi, Sensing ensembles for nitroaromatics, J, of Materials Chem. C., 6 (2018) 12142-12158.
24. L.E. Kreno, K. Leong, O.K. Farha, M. Allendorf, R.P. Van Duyne, J.T. Hupp, Metal-Organic Framework Materials as Chemical Sensors, Chem. Rev., 112 (2012) 1105-1125.
25. Z.C. Hu, B.J. Deibert, J. Li, Luminescent metal-organic frameworks for chemical sensing and explosive detection, Chem. Soc. Rev., 43 (2014) 5815-5840.
26. W.P. Lustig, S. Mukherjee, N.D. Rudd, A.V. Desai, J. Li, S.K. Ghosh, Metal-organic frameworks: functional luminescent and photonic materials for sensing applications. Chem. Soc. Rev., 46 (2017) 3242-3285.
27. A. Altun, E. Senkuytu, D. Davarci. Synthesis and crystal structure of the 6-oxyquinoline derivative cyclotriphosphazene chemosensor with high selectivity and immediate sensitivity for Fe(III) ion and TNT detection, Polyhedron, 240 (2023) 116458.
28. H. Zhu, TM. Geng, K.B. Tang, Fully Flexible Covalent Organic Frameworks for Fluorescence Sensing 2,4,6-Trinitrophenol and p-Nitrophenol. Polymers 15 (2023) 653.
29. K.K. Kartha, A. Sandeep, V.K. Praveen, A. Ajayaghosh, Detection of Nitroaromatic Explosives with Fluorescent Molecular Assemblies and π-Gels, Chem. Record., 15 (2015) 252-265.
30. F. Akhgari, H. Fattahi, Y.M. Oskoei. Recent advances in nanomaterial-based sensors for detection of trace nitroaromatic explosives, Sen. and Actuators B-Chem., 221 (2015) 867-878.
31. A. Kose, S. Erkan, M. Tümer. A series of phenanthroline-imine compounds: Computational, OLED properties and fluorimetric sensing of nitroaromatic compounds, Spectrochimica Acta Part a-Mol. and Biomol. Spec., 286 (2023) 122006.
32. N. Turan, K. Buldurun, F. Türkan, A. Aras, N. Çolak, M. Murahari, et al., Some metal chelates with Schiff base ligand: synthesis, structure elucidation, thermal behavior, XRD evaluation, antioxidant activity, enzyme inhibition, and molecular docking studies, Molecular Diversity, 26 (2022) 2459-2472.
33. D. Laziz, C. Beghidja, N. Baali, B. Zouchoune, A. Beghidja. Synthesis, structural characterization, DFT calculations and biological properties of mono- and dinuclear nickel complexes with tetradentate transformed ligands by aerobic oxidative-coupling reactions, Inorganica Chimica Acta, 497 (2019) 119085.
34. K. Buldurun. Synthesis, Characterization, Thermal Study and Optical Property Evaluation of Co(II), Pd(II) Complexes Containing Schiff Bases of Thiophene-3-Carboxylate Ligand, J. of Electronic Materials, 49 (2020) 1935-43.
35. M.E. Alkis, K. Buldurun, Y. Alan, N. Turan, A. Altun. Electroporation Enhances the Anticancer Effects of Novel Cu(II) and Fe(II) Complexes in Chemotherapy-Resistant Glioblastoma Cancer Cells, Chemistry & Biodiversity, 20 (2023).
36. Buldurun K, Özdemir M. Ruthenium(II) complexes with pyridine-based Schiff base ligands: Synthesis, structural characterization and catalytic hydrogenation of ketones, J. of Mol. Structure, 1202 (2020) 127266.
37. S.O. Tümay, S. Yesilot. Small molecule based water-soluble fluorescence material for highly selective and ultra-sensitive detection of TNT: Design and spectrofluorimetric determination in real samples, Sen. and Actuators B-Chem., 343 (2021) 130088.
38. C. Carrillo-Carrión, B.M. Simonet, M. Valcárcel, Determination of TNT explosive based on its selectively interaction with creatinine-capped CdSe/ZnS quantum dots, Anal. Chimica Acta, 792 (2013) 93-100.
39. Q. Zhang, D.M. Zhang, Y.L. Lu, Y. Yao, S. Li, Q.J. Liu, Graphene oxide-based optical biosensor functionalized with peptides for explosive detection, Biosensors & Bioelectronics, 68 (2015) 494-499.
40. J.R. Albani, Principles and Applications of Fluorescence Spectroscopy, Wiley-Blackwel Publisher, Lille, France 2007.
41. H.C. Hung, C.W. Cheng, Y.Y. Wang, Y.J. Chen, W.S. Chung, Highly Selective Fluorescent Sensors for Hg and Ag Based on Bis-triazole-Coupled Polyoxyethylenes in MeOH Solution. E. J. of Organic Chem., 36 (2009) 6360-6366.
42. V. Sharma, M.S. Mehata. Rapid optical sensor for recognition of explosive 2,4,6-TNP traces in water through fluorescent ZnSe quantum dots, Spectrochim. Acta Part a-Mol. and Biomol. Spec., 260 (2021) 119937.
43. S. Kumari, S. Joshi, T.C. Cordova-Sintjago, D.D. Pant, R. Sakhuja, Highly sensitive fluorescent imidazolium-based sensors for nanomolar detection of explosive picric acid in aqueous medium, Sen. and Actuators B-Chem, 229 (2016) 599-608.
44. X. Guo, B. Gao, X. Cui, J.H. Wang, W.Y. Dong, Q. Duan, et al., PL sensor for sensitive and selective detection of 2,4,6-trinitrophenol based on carbazole and tetraphenylsilane polymer, Dyes and Pigments, 191 (2021) 109379.